Extended Abstracts of the 2016 International Conference on Solid State Devices and Materials, Tsukuba, 2016, pp857-858

PS-9-11(Late News)

Electronic Band Structure of TiN/MgO nanostructures

Kazuaki Kobayashi[1], Hirokazu Takaki[1,2] , Masato Shimono[1], Nobuhiko Kobayashi[2], and Kenji Hirose[3]

[1] National Institute for Materials Science, *NOiC*, TIA, Namiki 1-1, Tsukuba, Ibaraki 305-0044, Japan
Phone: +81-29-860-4511 E-mail: KOBAYASHI.Kazuaki@nims.go.jp
[2] Univ. of Tsukuba, Institute of Applied Physics, *NOiC*, TIA, 1-1-1 Tennodai, Tsukuba, Ibaraki 305-8573, Japan
[3] NEC Corporation, Smart Energy Research Laboratories, 34 Miyukigaoka, Tsukuba, Ibaraki 305-8501, Japan

Abstract

Various nanostructured TiN(001)/MgO(001) superlattices based on a repeated slab model have been investigated by using the total energy pseudopotential method. The electronic states of the rectangular TiN dot/MgO(001)-2x2 and 3x3 superlattices are semiconducting. Their electronic properties depend on a shape of the TiN dot and a size of the MgO substrate.

1. Introduction

Nanostructured materials are focused on enhancing the thermoelectric properties [1-4]. We have investigated TiN(001)/MgO(001)-1x1 and related interfaces previously [5,6] in order to support experimental results [7] of the TiN thin film on a MgO substrate using molecular beam epitaxy. The electronic structures of all the TiN(001)/MgO(001)-1x1 superlattices correspond to metallicity [5,6]. Furthermore, we have calculated thermoelectric properties (Seebeck coefficients, thermal conductance, figure of merit [*ZT*]) of TiN(001)/MgO(001) superlattices along the *c*-axis using Non-equilibrium Green Function (NEGF) method [8] although *ZT* is quite small with approximately 0.002.

In this study, a TiN dot structure on a MgO substrate is considered as shown in Fig. 1. The main purpose of this study is to obtain nanostructured TiN dot/MgO superlattices which are structurally relaxed because our NEGF calculations [8,9] cannot relax them. Another important purpose is to search semiconducting nanostructured materials. A nonmetallic state is more suitable to enhance thermoelectric properties than a metallic state. Therefore, it is expected that small TiN dot structures on the large MgO substrates as 2x2 and 3x3 will be nonmetallic.

2. Method of Calculations

The present calculation is based on local density approximation (LDA) in density functional theory (DFT) [10,11] with the Wigner [12] formula for the exchange-correlation. The optimized pseudopotentials by Troullier and Martins (TM) [13,14] are used for Ti, Mg, N, and O. Nonlocal parts of the pseudopotentials are transformed to the Kleinman-Bylander separable forms [15] without ghost bands. A partial core correction (PCC) [16] is considered for the Ti and Mg pseudopotentials. The wave function is expanded in plane waves and the cutoff energies are 36 Ry, 49 Ry, 72.25 Ry, 81 Ry, and 144 Ry. The mesh sizes of the sampling k-points in the whole Brillouin zone (BZ) are 2x2x1 (49 Ry), 4x4x1 (36 Ry, 72.25 Ry), and 6x4x1 (81 Ry, 144 Ry). In this study, two TiN dot structures are considered. One is one Ti and one N atoms per layer as a rectangular shape and the other is two Ti and two N atoms per layer as a rectangular parallelepiped shape as shown in Fig. 1, schematically. All atoms in the supercell were fully relaxed.

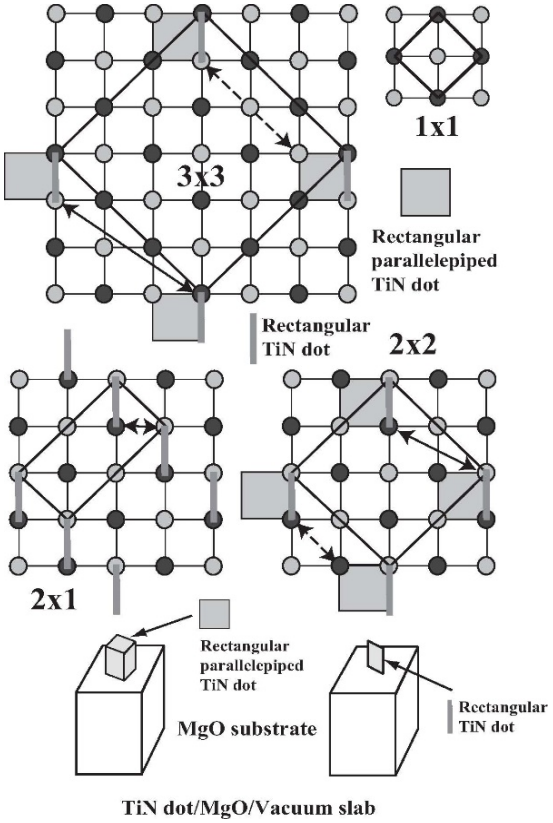

Fig. 1 Schematic top views of TiN dot/MgO-1x1, 2x1, 2x2, and 3x3 superlattices indicated by thick lines. Shaded stick and rectangular indicate “rectangular TiN dot” and “rectangular parallelepiped TiN dot”, respectively. Solid and dotted leftrightarrows indicate the nearest neighbor distances of rectangular and rectangular parallelepiped TiN dots, respectively. The bird’s-eye views of rectangular parallelepiped and rectangular TiN dot/MgO superlattices (two-layer TiN, six-layer MgO, and four-layer vacuum) are also depicted.

3. Results and Discussion

The rectangular TiN dot/MgO-2x1 superlattice corresponds to metallicity. In contrast, the rectangular TiN dot/MgO-2x2 superlattice corresponds to semiconductor. The electronic band structure of the rectangular TiN dot/MgO-2x2 superlattice is shown in Fig. 2 (upper panel).

From this figure, the valence band maximum and conduction band minimum around the band gap are dispersive. There are two flat (= localized) bands below the valence band maximum with approximately 2.5 eV and they do not contribute to the conductivity. A lower panel in Fig. 2 is the electronic band structure of the rectangular parallelepiped TiN dot/MgO-2x2 superlattice, and it corresponds to metallicity. As the same way of the 2x2 cases, the electronic state of the rectangular TiN dot/MgO-3x3 superlattice is semiconducting and that of the rectangular parallelepiped TiN dot/MgO-3x3 superlattice is metallic.

The band gap value in the rectangular TiN dot/MgO-2x2 (3x3) superlattice is approximately 0.18 eV (0.54 eV). Although it could be underestimated the band gap value due to inaccuracy of the DFT-LDA calculation, the band gap value of the rectangular TiN dot/MgO-3x3 is larger than the 2x2 case. Consequently, the electronic state of the TiN dot/MgO superlattice depends on its dot shape and the size of MgO substrate. Furthermore, the band gap value of the TiN dot/MgO superlattice could be controllable to vary its MgO substrate size.

4. Conclusions

We have calculated the internal lattice and electronic properties of various TiN dot/MgO superlattices using the total energy pseudopotential method. The electronic properties (electronic band structure, DOS) of the various TiN dot/MgO superlattices have been definitively established in this study. The electronic structures of all rectangular parallelepiped TiN dot/MgO superlattices correspond to metallicity. In contrast, the electronic structures of rectangular TiN dot/MgO-2x2 and 3x3 superlattices are non-metallic. Their band gap values are 0.18 eV (2x2) and 0.54 eV (3x3). The electronic state of each TiN dot/MgO superlattice depends on the shape of the TiN dot and the size of the MgO substrate.

Acknowledgements

We would like to extend our thanks to Dr. T. Mori of NIMS for continual support. This study is supported by the Materials for Thermal Energy Conversion Open Laboratory, *NOiC*, TIA. The numerical calculations were performed using Z420 and Z620 workstations (HP), and the numerical materials simulator [Altix, SGI] in NIMS.

References

[1] L. D. Hicks and M. S. Dresselhaus, Phys. Rev. B**47** (1993) 12727.

[2] L. D. Hicks and M. S. Dresselhaus, Phys. Rev. B**47** (1993) 16631.

[3] J. O. Sofo and G. D. Mahan, Appl. Phys. Lett. **65** (1994) 2690.

[4] A. J. Minnich, M. S. Dresselhaus, Z. F. Ren, and G. Chen, Energy Environ. Sci. **2** (2009) 466.

[5] K. Kobayashi, N. Kobayashi, and K. Hirose, *e-J. Surf. Sci. Nanotech.*, **12** (2014) 230.

[6] K. Kobayashi, H. Takaki, N. Kobayashi, and K. Hirose, JPS Conf. Proc. **5** (2015) 011013.

[7] I. Ohkubo, T. Aizawa, and T. Mori, private communications.

[8] H. Takaki, K. Kobayashi, M. Shimono, N. Kobayashi, and K. Hirose, J. Appl. Phys. **119** (2016) 014302.

[9] K. Hirose, K. Kobayashi, M. Shimono, H. Ishii, and N. Kobayashi, *e-J. Surf. Sci. Nanotech.*, **12** (2014) 115.

[10] P. Hohenberg and W. Kohn, Phys. Rev. **136** (1964) B864.

[11] W. Kohn and L. J. Sham, Phys. Rev. **140** (1965) A1133.

[12] E. P. Wigner: Phys. Rev. **46** (1934) 1002.

[13] N. Troullier and J. L. Martins: Phys. Rev. B **43** (1991) 1993.

[14] K. Kobayashi, Mater. Trans. **42** (2001) 2153.

[15] L. Kleinman and D. M. Bylander, Phys. Rev. Lett. **48** (1982) 1425.

[16] S. G. Louie, S. Froyen, and M. L. Cohen, Phys. Rev. B **26** (1982) 1738.

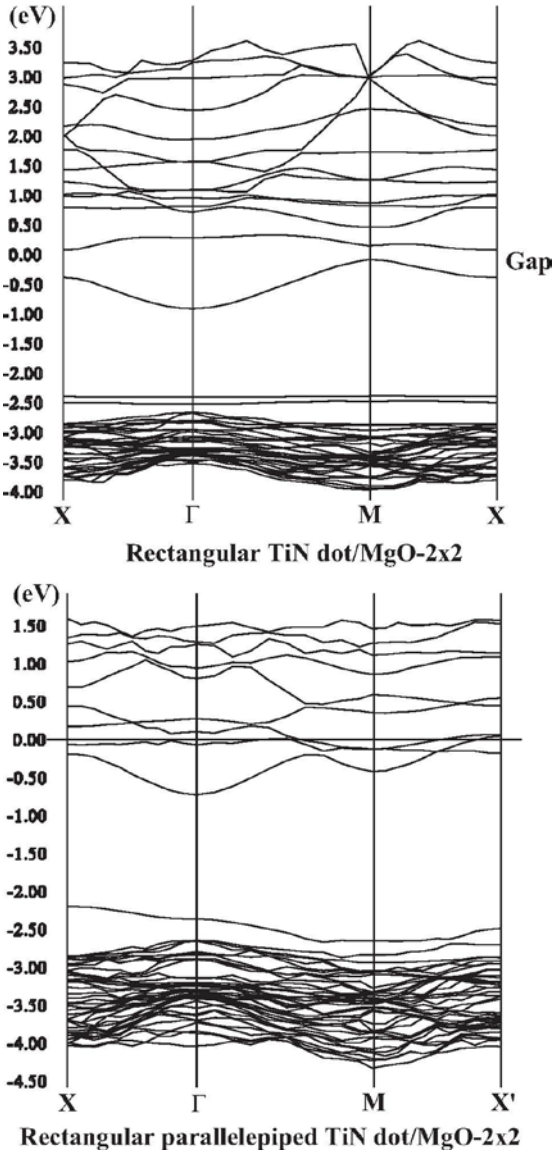

Fig. 2 Upper panel is the electronic band structure of the rectangular TiN dot/MgO-2x2 superlattice. "Gap" indicates the narrow band gap. Lower panel is the electronic band structure of the rectangular parallelepiped TiN dot/MgO-2x2 superlattice. The Fermi level is indicated by the horizontal line. The *X* point is not equal to the *X'* point.